PHYSICAL REVIEW C **107**, 044315 (2023)

Shape isomers of α-like nuclei in terms of the multiconfigurational dynamical symmetry

Phong Dang [*]
Institute for Nuclear Research, 4001 Debrecen, P. O. Box 51, Hungary
and Faculty of Science and Technology, University of Debrecen, Debrecen, Hungary

Gábor Riczu [†] and József Cseh [‡]
Institute for Nuclear Research, 4001 Debrecen, P. O. Box 51, Hungary

(Received 15 March 2023; accepted 5 April 2023; published 19 April 2023)

Background: The shape isomers of the $N = Z =$ even nuclei are known from the energy-surface calculations within the Bloch-Brink (BB) α-cluster model and Nilsson model. As an alternative, a new method (called SCS) has been proposed recently for determining the stable shapes, which is based on the investigation of the stability and consistency of the SU(3) symmetry (or quadrupole deformation).
Purpose: We wish to derive the shape isomers of the α-like nuclei from the SCS method and compare them with the results of the energy-surface calculation. Furthermore, we intend to study the consequences of the stable symmetries. In particular, we investigate (i) what kind of binary clusterizations are structurally allowed for the shape isomers and (ii) if energy spectra similar to those of the BB model can be obtained with a simple dynamically symmetric Hamiltonian.
Methods: We determine the stability and self-consistency of the quadrupole deformation from a systematic calculation with the Nilsson model by applying the concept of the quasidynamical U(3) symmetry. The allowed cluster configurations are determined from the application of the U(3) and $\text{U}^{\text{ST}}(4)$ selection rules. The forbidden ones are characterized quantitatively. The energy spectrum is calculated with a simple dynamically symmetric Hamiltonian of the multiconfigurational dynamical symmetry (MUSY), which proved to be useful for the description of some experimental spectra.
Results: The shape isomers found from the SCS method are in good agreement with the results of the energy surface method (BB and Nilsson models). Their allowed binary clusterizations are obtained from structural selection rules, but they give a hint for the available reaction channels, too. Last, a very simple energy functional is able to reproduce the gross features of their energy spectra in a large range of excitation energy and deformation.
Conclusions: The similarity of the shape isomers from two very different methods gives a strong support to these predictions. The reasonable reproduction of the energy distribution of the "ground-band heads" is especially remarkable, considering the fact that MUSY is able to produce the complete spectra in detail, not only the energy minima.

DOI: 10.1103/PhysRevC.107.044315

I. INTRODUCTION

The appearance of different stable shapes (shape isomers) in many-body systems is a frequent phenomenon, and their investigation attracts much attention both from the experimental and from the theoretical sides. In atomic nuclei the ground states usually have a moderate deformation, but in several cases superdeformed states have been observed. They have an approximately ellipsoidal shape of major axes with ratio 2:1:1. Experimental evidence seems to accumulate also for hyperdeformed states (of ratio 3:1:1). Theoretical studies predict more exotic configurations as well, e.g., linear chain of α particles in $N = Z =$ even nuclei.

Recently, symmetry-related studies added interesting new aspects to this topic. One of them is the discovery of emergent symmetries. In particular, approximately valid SU(3) and symplectic symmetries were found from large-scale calculations which were carried out with nonsymmetric interactions [1–4]. Both model interactions as well as realistic nucleon-nucleon forces were applied in these studies. The symmetry diagnostics of the wave function revealed that the SU(3) and symplectic symmetries are valid to a good approximation. This is a surprising finding, considering that no symmetry-related model assumptions are assumed. Especially remarkable is the presence of these symmetries in *ab initio* calculations, when all nucleons are treated uniformly, and realistic nucleon-nucleon forces govern their behavior. These results led to the conclusion that the nuclear dynamics is

---

[*] dqphong21@gmail.com
[†] riczugabor@atomki.hu
[‡] cseh@atomki.hu

dominated by a few stable deformations [3,4], with vibrational excitations.

The understanding of the interrelation between fundamental structure models has also been deepened recently by the discovery of a connecting dynamical symmetry, called MUSY. This symmetry bridges the shell, collective, and cluster models to each other [5,6] for the multi-major-shell problem. Since MUSY plays an important role in our study, we briefly summarize its basic features in the next section. Here we just mention that it has several interesting applications with remarkable predictive power.

In this work we derive the shape isomers of the α-like nuclei from the study of the stability and self-consistency of the U(3) [or SU(3)] symmetry, or since it is uniquely related to the quadrupole deformation [7], one can say from the stability and self-consistency of the deformation. This method is called SCS, abbreviating stability and consistency of the SU(3) symmetry, and it is an alternative to the usual energy-minimum calculation. The U(3) symmetry, which is investigated in SCS [8], connects the shell and collective models (as it is discussed more in detail later). The calculations are based on the Nilsson model, which includes symmetry-breaking interactions, too. Therefore, the stable shapes revealed by our SCS method are examples of emergent symmetries, too.

The most systematic search for the stable shapes of the α-like nuclei was carried out within the framework of the Bloch-Brink α-cluster model [9–11] and the Nilsson model [12]. We compare our results with these ones.

We determine also the allowed binary clusterizations of the shape isomers by applying (microscopic) U(3) and $\mathrm{U}^{\mathrm{ST}}(4)$ selection rules. Since the cluster configurations are closely related to reaction channels (one can say that they are actually defined by reaction channels), the determination of the allowed clusterizations carries important information on the reactions which can populate the shape isomers.

Owing to the effect of the antisymmetrization, different cluster configurations can have large overlap with each other or with the shell configuration. In some cases the overlap can be complete, that is 100%. For the U(3) basis states of the different configurations, this total overlap can be picked up easily, and we do so. Hence, we select those configurations which are identical with each other [up to the validity of the U(3) symmetry, which turns out to be a good approximation].

The energy spectra of shape isomers are obtained from a dynamically symmetric Hamiltonian of MUSY, which proved to be useful in describing experimental data. In particular, it could reproduce the gross features of the spectra of different configurations (shell, or quartet, core-plus-α, heavy clusters) in a wide range of energy and deformation [5,6,13–15]. Here we address the question if this simple energy functional is able to produce spectra similar to those of the BB cluster model, which contain many local energy minima. The MUSY applications to energy spectra incorporated so far two [5,14] or three valleys [13,15]. It is worth noting, however, that MUSY gives full spectra, not only the energy minima, and in some cases a detailed spectrum of heavy-ion resonances [14] or α particles [16] could be obtained as a parameter-free prediction in good agreement with the observation. Here we wish to reveal if the simple dynamically symmetric Hamiltonian (with two or three parameters) is capable of reproducing the location of many minima of an energy surface.

In what follows first we summarize some characteristics of MUSY in Sec. II, and then we determine the shape isomers of α-like nuclei from the SCS method, based on the Nilsson model and the concept of quasidynamical symmetry in Sec. III. The results are compared with those of the energy-surface calculations, based on the Nilsson and the α-cluster models. The possible binary clusterizations of the shape isomers are obtained in Sec. IV, and Sec. V contains some discussion on the cluster-shell coexistence. The energy spectra are presented in Sec. VI. Finally the conclusions are drawn in Sec. VII.

II. MULTICONFIGURATIONAL DYNAMICAL SYMMETRY

The key role of the SU(3) symmetry in connecting the spherical shell model, the quadrupole collective model and the cluster model is known since 1958 [17–19]. First the connection was found for the single-shell problem. In short we can say that their common intersection is provided by the

$$\mathrm{U}(3) \supset \mathrm{SU}(3) \supset \mathrm{SO}(3) \tag{1}$$

dynamical symmetry.

It took a long time until symmetry-governed models for the multi-major-shell problem were developed in the shell [20,21], collective [22,23], and cluster [24,25] pictures, and their connection was revealed [5,6]. It turns out that the intersection of these fundamental models is given by a dynamical symmetry that is a generalization of the previous one:

$$\mathrm{U}_s(3) \otimes \mathrm{U}_e(3) \supset \mathrm{U}(3) \supset \mathrm{SU}(3) \supset \mathrm{SO}(3), \tag{2}$$

called multiconfigurational dynamical symmetry (MUSY). Here $\mathrm{U}_s(3)$ indicates the symmetry of valence shell in the shell and (microscopic) collective model, and the internal cluster symmetry in the cluster model, while $\mathrm{U}_e(3)$ stands for major shell excitation (meaning relative motion in the cluster picture). A further symmetry in the particle-index pseudospace connects the different configurations with each other and can guide us to derive physical operators that are invariant with respect to the connecting transformations [5]. Therefore, MUSY is a composite symmetry of composite systems. The systems contain two or more configurations, each of them shows a dynamical symmetry of type (2), and a further symmetry connects the different components to each other.

An interesting feature of MUSY is that it shows a dual breaking of symmetries: the larger U(3) and SU(3) symmetries are broken dynamically, due to the presence of symmetry-breaking interactions (see below), while the rotational SO(3) symmetry is spontaneously broken in the eigenvalue problem of the intrinsic Hamiltonian [26]. The spontaneous breaking results in deformed shape in the intrinsic system: quadrupole deformation in the shell model and more exotic molecular shape in the cluster model. This kind of dual breaking of symmetries is a common feature of many dynamical symmetries of the algebraic structure models [27], including the Elliott model, as their prototype [17].

III. SHAPE ISOMERS

A. Method of calculation

Here we employ the SU(3) symmetry to explore the possible shape isomers of 4N-nuclei (with $N = 3, 4, \ldots, 11$) by examining the stability and self-consistency of the quadrupole deformation parameters.

Note that the SU(3) here is a quasidynamical (or effective) symmetry [28–30], a generalization of the original SU(3) applied by Elliot [17], and it is more broadly usable compared to the simple one. The latter is known to be valid for the ground-state region of light nuclei. At the excited states where the real SU(3) is not well defined, one has to utilize the quasidynamical symmetry. Nevertheless, whenever the simple symmetry is valid, both of the symmetries coincide.

The method of calculation is developed from the observation that the asymptotic Nilsson-state of the many-nucleon system is an intrinsic state of the quasidynamical SU(3) symmetry [30]. Originally, the method was defined for large prolate deformation [30], and later it was extended to the oblate side as well as to small deformations [31]. The details are discussed in Ref. [8], and here we summarize merely the basic steps.

(1) Derive the asymptotic Nilsson states by solving the eigenvalue problem of the deformed but cylindrically symmetric Hamiltonian,

$$H = -\frac{\hbar^2}{2M}\Delta + \frac{M}{2}\left[\omega_\perp^2(x^2+y^2)+\omega_z^2 z^2\right] - C(\vec{l}\cdot\vec{s}) - D\vec{l}^2,$$

where the last two terms are due to the spin-orbit interaction and angular momentum. The elongation parameter

$$\epsilon = \frac{\omega_\perp - \omega_z}{\omega_0} \text{ with } \omega_z = \omega_0\left(1-\frac{2}{3}\epsilon\right),$$
$$\omega_\perp = \omega_0\left(1+\frac{1}{3}\epsilon\right)$$

is related to the more common deformation parameter β by $\epsilon \approx 0.95\beta$ [8].

(2) Determine the Nilsson orbitals as a function of the quadrupole deformation parameters and then obtain the many-particle state by filling them with nucleons following the energy-minimum and Pauli exclusion principles.

(3) Diagonalize the deformed Hamiltonian of a triaxial shape with the deformed harmonic oscillator potential,

$$V = \frac{M}{2}\left(\omega_x^2 x^2 + \omega_y^2 y^2 + \omega_z^2 z^2\right), \tag{3}$$

in cylindrical coordinates. Thereafter, expand the Nilsson orbitals of a given deformation (ϵ, γ) in terms of the asymptotic Nilsson states derived previously [31].

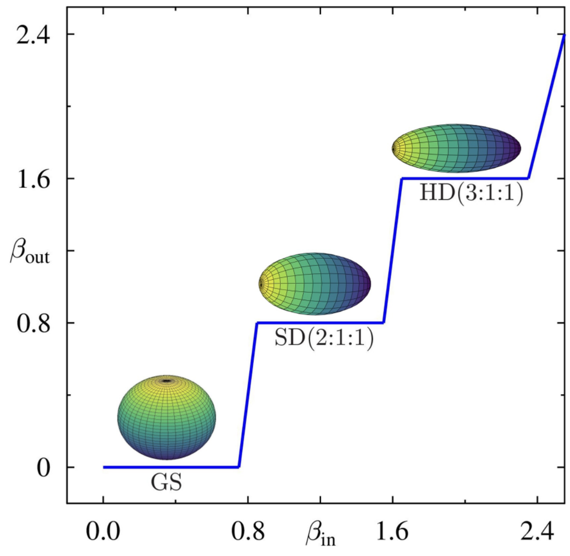

FIG. 1. A schematic illustration of finding stable shape isomers based on the stability and self-consistency of the SU(3) symmetry.

(4) Determine the effective SU(3) quantum numbers (λ, μ) from the linear combinations of the single particle orbitals and from the relations of the large deformation [30].

(5) These effective quantum numbers can be converted to the quadrupole deformation parameters [32],

$$\beta^2 = \frac{16\pi}{5N_0^2}(\lambda^2+\mu^2+\lambda\mu),\ \gamma = \arctan\frac{\sqrt{3}\mu}{2\lambda+\mu}, \tag{4}$$

where $N_0 = n_1 + n_2 + n_3 + \frac{3}{2}(A-1)$ with A as the mass number of the nucleus is the number of oscillator quanta, n_1, n_2, n_3 are U(3) quantum numbers related to the SU(3) counterparts by $\lambda = n_1 - n_2$ and $\mu = n_2 - n_3$. Thereby, one can examine the stability and self-consistency of both the effective SU(3) quantum numbers and the deformation parameters.

B. Stable shapes

Constructing graphs of the output parameters as a function of the input ones, we witness a pattern of step functions, a schematic demonstration is given in Fig. 1. The shape isomers associated with U(3) quantum numbers $[n_1, n_2, n_3]$ are determined in the plateauing zones, shown in Figs. 2 and 3. Note that the major axes of the ellipsoidal shape of the nucleus can be characterized by the SU(3) quantum numbers as follows:

$$\frac{a}{c} = \frac{n_1+\frac{A}{2}}{n_3+\frac{A}{2}} \quad\text{and}\quad \frac{b}{c} = \frac{n_2+\frac{A}{2}}{n_3+\frac{A}{2}}. \tag{5}$$

The results demonstrate a strong concurrence with the configurations calculated by the Bloch-Brink cluster model in Refs. [9–11]. A comparison between the SCS and energy-surface calculation, including the Nilsson model [12] as well, is given in Table I.

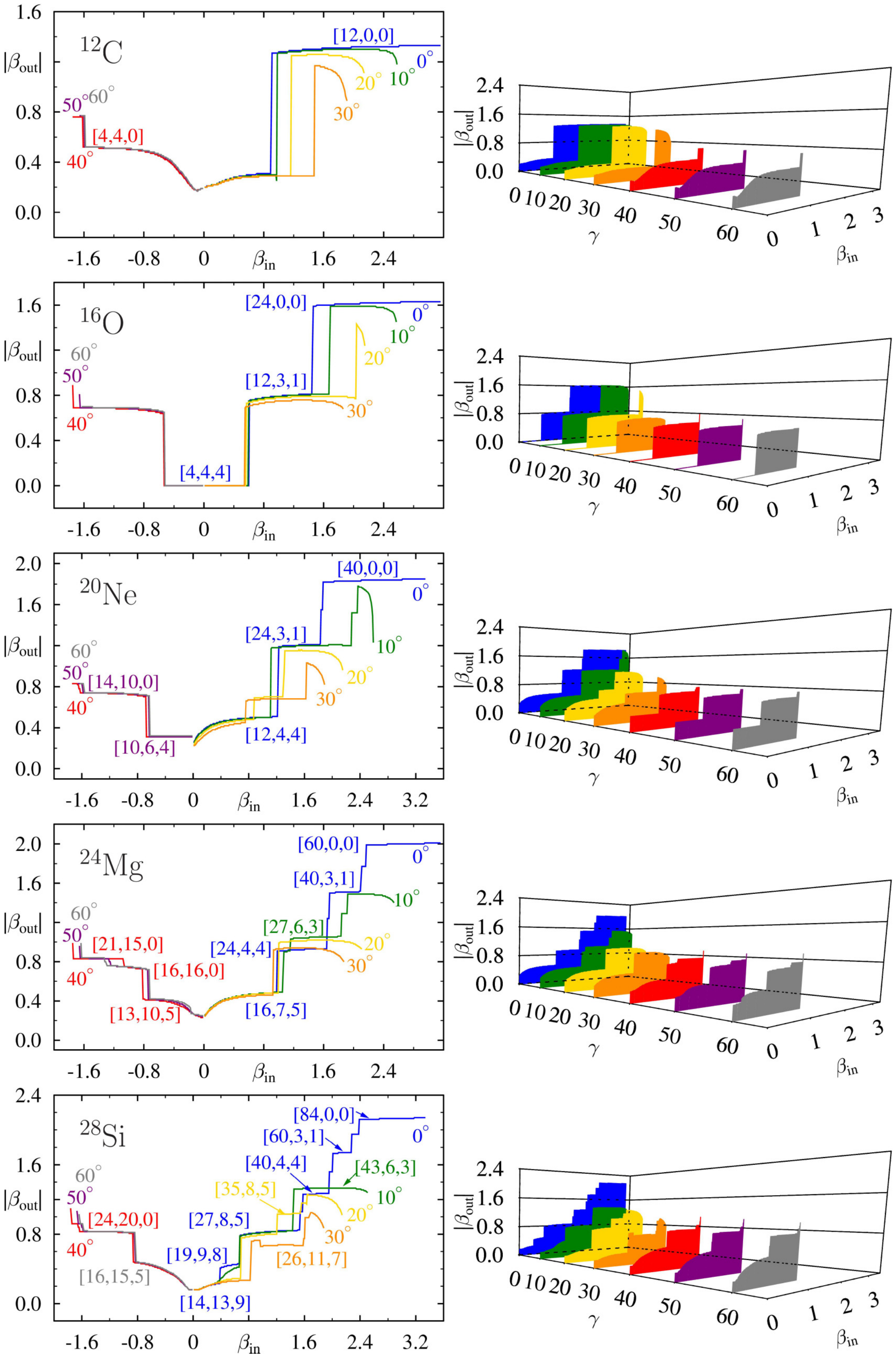

FIG. 2. Shape isomers given by the U(3) quantum numbers $[n_1, n_2, n_3]$ of some 4N-nuclei obtained from the stability and self-consistency of the quasidynamical SU(3) symmetry. The calculation is carried out for different values of the deformation parameter γ with step of 10°.

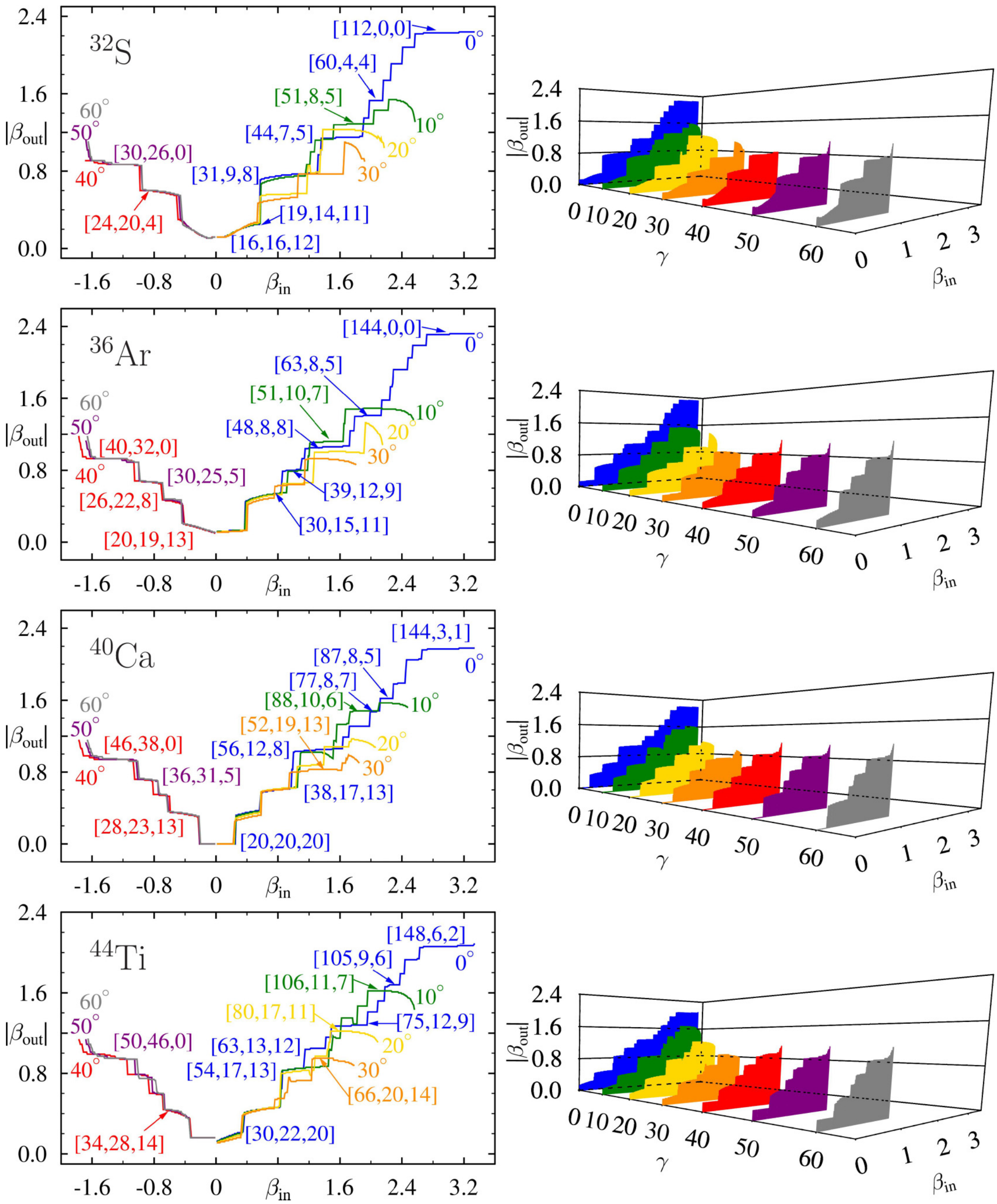

FIG. 3. Analogous to Fig. 2.

IV. CLUSTERIZATION OF THE SHAPE ISOMERS

Here we explore the possible binary clusterizations of the shape isomers aforenamed. In particular, we examine all possible combinations of two stable nuclei (^{8}Be is, despite being unstable, included for systematic purpose). We apply the U(3) selection rule for the space part and the spin-isospin U(4) selection rule for the other degrees of freedom. In this consideration, the clusters are supposed to be in their intrinsic ground state, as the corresponding (free) nuclei. As for the shape and orientation of the clusters are concerned, no restriction is applied. Arbitrary quadrupole deformation and relative orientation are allowed.

The U(3) selection rule (which can be applied also for multicluster systems [33]) for a binary clusterization requires

$$[n_1, n_2, n_3] = \left[n_1^A, n_2^A, n_3^A\right] \otimes \left[n_1^B, n_2^B, n_3^B\right] \otimes [n^R, 0, 0], \quad (6)$$

where $[n_1, n_2, n_3]$ is the U(3) irreducible representation (*irrep*) of the parent nucleus, while the first two factors on the right-hand side are the U(3) *irreps* of the two clusters and the last one stems from the relative motion.

The U(3) selection rule copes with space symmetry, and hence it is possible to quantitize the geometrical difference between the quadrupole shapes of the combination of the two clusters (with their relative motion) and of the parent nucleus

TABLE I. Comparison of shape isomers discovered by the Nilsson energy surface calculation [12], the Bloch-Brink (BB) (α-cluster) model [9–11], and by the stability and self-consistency of the SU(3) symmetry (SCS) [8]. For the first, the ratio of harmonic frequencies $\omega_{x:y:z} = \omega_x : \omega_y : \omega_z$ is given with the deformation parameters. Meanwhile, for the second, the α configuration of each state, the corresponding shell configuration, its excitation energy E(MeV), and the U(3) quantum numbers $[n_1, n_2, n_3]$ derived from the configuration are provided. The abbreviations of the α configurations are the following: GS for ground state, α-ch for the linear α chain, e.tri for equilateral triangle, ttrh for tetrahedral shape, bpy for bipyramidal, a.bpy for asymmetric bipyramid, tri for triaxial, h.tri for highly deformed triaxial, pro for prolate, ob for oblate, h.ob for highly deformed oblate. The notation 2D(○ : ○) implies a two-dimensional configuration with $\omega_y : \omega_x$ given in the parentheses. Last, for the SCS method, the results are given as U(3) quantum numbers, and the deformation parameters. The abbreviations in the names of the discovered shape isomers are: GS for ground state, α-ch for the linear α chain, SD for superdeformed state, HD for hyperdeformed state, Tri for triaxial, Pr for prolate, Ob for oblate, VP for very deformed prolate, EP for extreme prolate, and asym for asymmetric; in some cases, the subscripts appear and their values are $\hbar\omega$.

		Energy surface		Bloch-Brink α-cluster model				SCS method			
Nucl.	$\hbar\omega$	$\omega_{x:y:z}$	(γ,ϵ)	α-conf.	Shell conf.	E	U(3)	Shape	U(3)$_{\text{eff}}$	(γ,ϵ)	$a:b:c$
^{12}C	0	2:1:1	(60,0.83)	GS$_{\text{e.tri}}$	$(1)^{-4}$	0.00	[4,4,0]	GS(Ob)	[4,4,0]	(60,0.5)	1.7:1.7:1
	4	3:3:1	(0,1.11)	α-ch	$(1)^4(2)^4$	7.90	[12,0,0]	α-ch	[12,0,0]	(0,1.3)	3:1:1
^{16}O	0	1:1:1	(0,0)	GS$_{\text{ttrh}}$	$(1)^{12}$	0.00	[4,4,4]	GS	[4,4,4]	(0,0)	1:1:1
	4	4:2:1	(43,1.04)	kite	$(1)^{-4}[20]^4$	17.41	[12,4,0]	SD	[12,3,1]	(9.8,0.8)	2.2:1.2:1
	12	4:4:1	(0,1.2)	α-ch	$(1)^4(2)^4(3)^4$	18.90	[24,0,0]	α-ch	[24,0,0]	(0,1.6)	4:1:1
^{20}Ne	0	2:2:1	(0,0.4)	GS$_{\text{bpy}}$	$[200]^4$	0.00	[12,4,4]	GS	[12,4,4]	(0,0.5)	1.6:1:1
	0			a.bpy[a]	$[200]^4$	1.60	[12,4,4]	asym	[10,6,4]	(19.1,0.3)	1.4:1.1:1
	4	8:3:2	(50,1.17)	2D(3:2)	$(1)^{-4}[20]^4[11]^4$	20.03	[16,8,0]	SD(Tri)	[14,10,0]	(43.9,0.7)	2.4:2:1
	8			2D(3:1)	$(1)^{-4}[20]^4[30]^4$	24.98	[24,4,0]	HD	[24,3,1]	(4.5,1.2)	3.1:1.2:1
	20	5:5:1	(0,1.25)	α-ch	$(1)^4(2)^4(3)^4(4)^4$	31.70	[40,0,0]	α-ch	[40,0,0]	(0,1.8)	5:1:1
^{24}Mg	0	4:3:2	(20,0.45)	GS$_{\text{tri}}$	$[200]^4[101]^4$	0.00	[16,8,4]	GS	[16,7,5]	(9.8,0.5)	1.6:1.1:1
	0							Tri$_0$	[13,10,5]	(38.2,0.3)	1.5:1.3:1
	4		(0,1.0)	pro	$[200]^4[300]^4$	14.18	[24,4,4]	SD(Pr)	[24,4,4]	(0,0.9)	2.2:1:1
	4	3:1:1	(60,1.23)	2D(1:1)[b]	$(1)^{-4}[20]^4[11]^4[02]^4$	24.94	[16,16,0]	SD(Ob)	[16,16,0]	(60,0.7)	2.3:2.3:1
	4			triangle[b]	$(1)^{-4}[20]^4[11]^4[02]^4$	27.22	[16,16,0]				
	8	5:2:1	(42,1.26)	2D(2:1)	$(1)^{-4}[20]^4[11]^4[30]^4$	25.68	[28,8,0]	Tri$_8$	[27,6,3]	(6.6,1)	2.6:1.2:1
	8							Ob$_8$	[21,15,0]	(43.9,0.8)	2.8:2.2:1
	16							HD	[40,3,1]	(2.6,1.5)	4:1.2:1
	32	6:6:1	(0,1.25)	α-ch	$(1)^4(2)^4(3)^4(4)^4(5)^4$	45.50	[60,0,0]	α-ch	[60,0,0]	(0,1.9)	6:1:1
^{28}Si	0							Ob$_0$	[14,13,9]	(49,0.19)	1.2:1.2:1
	0	3:3:2	(0,0.45)	GS(pro)	$[200]^4[110]^4[101]^4$	0.00	[20,8,8]	Pr$_0$	[19,9,8]	(4.7,0.4)	1.5:1.0:1
	0	2:1:1	(60,0.49)	ob	$[200]^4[110]^4[020]^4$	2.40	[16,16,4]	GS	[16,15,5]	(55.3,0.4)	1.6:1.5:1
	4			tri	$[200]^4[110]^4[300]^4$	12.70	[28,8,4]	Tri$_4$	[27,8,5]	(7.2,0.8)	2.2:1.2:1
	8			h.ob	$(1)^{-4}[20]^4[11]^4[02]^4[21]^4$	32.27	[24,20,0]	Ob$_8$	[24,20,0]	(51.1,0.8)	2.7:2.4:1
	8			2D(3:2)	$(1)^{-4}[20]^4[11]^4[02]^4[30]^4$	38.85	[28,16,0]	Tri$_8$	[26,11,7]	(11.5,0.6)	1.9:1.2:1
	8		(60,1.35)								
	12		(0,1.0)	pro	$[200]^4[300]^4[400]^4$	26.20	[40,4,4]	HD	[40,4,4]	(0,1.2)	3:1:1
	12			tri	$(1)^{-4}[20]^4[11]^4[30]^4[21]^4$	37.37	[36,12,0]	Tri$_{12}$	[35,8,5]	(5.2,1)	2.6:1.2:1
	16	6:3:1	(35,1.32)					VP$_{16}$	[43,6,3]	(3.9,1.3)	3.4:1.2:1
	28							EP$_{28}$	[60,3,1]	(1.7,1.7)	4.9:1.1:1
	48			α-ch	$(1)^4(2)^4(3)^4(4)^4(5)^4(6)^4$	60.20	[84,0,0]	α-ch	[84,0,0]	(0,2)	7:1:1
^{32}S	0							Ob$_0$	[16,16,12]	(60,0.1)	1.1:1.1:1
	0	5:4:3	(20,0.21)	GS$_{\text{tri}}$	$[011]^{-4}[002]^{-4}$	0.00	[20,16,8]	GS	[19,14,11]	(21.8,0.2)	1.3:1.1:1
	0			pro	$[020]^{-4}[002]^{-4}$	4.30	[20,12,12]				
	4	2:2:1	(0,0.68)	S(2:1)[c]	$[200]^4[101]^4[110]^4[300]^4$	3.20	[32,8,8]	SD(Pr)	[31,9,8]	(2.2,0.7)	2:1:1
	4			h.ob	$[200]^4[110]^4[020]^4[210]^4$	13.40	[24,20,4]	SD(Ob)	[24,20,4]	(49.1,0.6)	2:1.8:1
	12			2D(3:2)	$(1)^{-4}[20]^4[11]^4[02]^4[30]^4[21]^4$	43.10	[36,20,0]	Tri	[36,20,0]	(33.7,0.9)	3.2:2.2:1
	12	10:3:2	(54,1.42)								
	12		(0,1.0)					HD$_{12}$	[44,7,5]	(2.6,1.1)	2.9:1.1:1
	20		(30,1.3)	2D(4:1)	$(1)^{-4}[20]^4[11]^4[21]^4[30]^4[40]^4$	45.69	[52,12,0]	HD$_{20}$	[51,8,5]	(3.3,1.2)	3.2:1.1:1
	24			pro	$[200]^4[300]^4[400]^4[500]^4$	45.50	[60,4,4]	EP$_{24}$	[60,4,4]	(0,1.5)	3.8:1:1
	68			α-ch	$(1)^4(2)^4(3)^4(4)^4(5)^4(6)^4(7)^4$	75.50	[112,0,0]	α-ch	[112,0,0]	(0,2.1)	8:1:1

TABLE I. (*Continued.*)

		Energy surface		Bloch-Brink α-cluster model				SCS method			
Nucl.	$\hbar\omega$	$\omega_{x:y:z}$	(γ,ϵ)	α-conf.	Shell conf.	E	U(3)	Shape	U(3)$_{\mathrm{eff}}$	(γ,ϵ)	$a:b:c$
^{36}Ar	0	3:2:2	(60,0.29)	GS(ob)	$(2)^{-4}$	0.00	[20,20,12]	GS	[20,19,13]	(52.4,0.2)	1.2:1.2:1
	4							Ob$_4$	[26,22,8]	(47.8,0.5)	1.7:1.5:1
	4			h.tri	$[200]^4[110]^4[101]^4[020]^4[300]^4$	16.80	[32,16,8]	Pr$_4$	[30,15,11]	(11.5,0.5)	1.7:1.1:1
	8		(7,0.74)					SD(Pr)	[39,12,9]	(5.2,0.8)	2.1:1.1:1
	8							SD(Ob)	[30,25,5]	(49.1,0.6)	2.1:1.9:1
	12			h.tri	$[200]^4[110]^4[101]^4[300]^4[400]^4$	24.00	[48,8,8]	SD$_{12}$	[48,8,8]	(0,1)	2.5:1:1
	16			2D(4:1)[d]	$(1)^{-4}[20]^4[11]^4[02]^4[30]^4[21]^4[12]^4$	63.00	[40,28,0]				
	16		(55,1.45)								
	16							HD(Pr)	[51,10,7]	(3.5,1.1)	2.8:1.1:1
	20		(47,1.33)	2D(2:1)	$(1)^{-4}[20]^4[11]^4[02]^4[30]^4[21]^4[40]^4$	62.71	[52,20,0]				
	20							HD(Ob)	[40,32,0]	(49.1,0.9)	3.2:2.8:1
	24							EP$_{24}$	[63,8,5]	(2.6,1.3)	3.5:1.1:1
	28			2D(3:1)	$(1)^{-4}[20]^4[11]^4[30]^4[21]^4[40]^4[31]^4$	69.52	[64,16,0]				
	92			α-ch	$(1)^4(2)^4(3)^4(4)^4(5)^4(6)^4(7)^4(8)^4$	91.30	[144,0,0]	α-ch	[144,0,0]	(0,2.2)	9:1:1
^{40}Ca	0	1:1:1	(0,0)	GS$_{\mathrm{ttrh}}$[e]	$(2)^{24}$	0.00	[20,20,20]	GS	[20,20,20]	(0,0)	1:1:1
	4	7:5:4	(50,0.45)					Ob$_4$	[28,23,13]	(40.9,0.3)	1.5:1.3:1
	8							SD(Pr)	[38,17,13]	(8.6,0.6)	1.8:1.1:1
	12							SD(Ob)	[36,31,5]	(51.4,0.7)	2.2:2:1
	16		(5,0.84)	b(3D)[f]	$[200]^4[110]^4[101]^4[300]^4[210]^4$ $[400]^4$	38.10	[56,12,8]	HD(Pr)	[56,12,8]	(4.3,1)	2.7:1.1:1
	20			2D(1:1)[g]	$(1)^{-4}[20]^4[11]^4[02]^4[30]^4[21]^4[12]^4$ $[03]^4$	95.33	[40,40,0]				
	20		(60,1.5)								
	24							HD(Ob)	[46,38,0]	(50.6,0.9)	3.3:2.9:1
	24			2D(3:2)[h]	$(1)^{-4}[20]^4[11]^4[02]^4[30]^4[21]^4[12]^4$ $[40]^4$	91.29	[56,28,0]	Pr$_{24}$	[52,19,13]	(8.2,0.8)	2.2:1.2:1
	32			2D(5:2)	$(1)^{-4}[20]^4[11]^4[02]^4[30]^4[21]^4[40]^4$ $[50]^4$	98.64	[72,20,0]	EP$_{32}$	[77,8,7]	(0.7,1.4)	3.6:1:1
	40			2D(4:1)	$(1)^{-4}[20]^4[11]^4[30]^4[21]^4[40]^4[31]^4$ $[50]^4$	99.69	[84,16,0]	EP$_{40}$	[87,8,5]	(1.8,1.5)	4.3:1.1:1
	44							EP$_{44}$	[88,10,6]	(2.5,1.5)	4.2:1.2:1
	88							EP$_{88}$	[144,3,1]	(0.7,2.1)	7.8:1.1:1
	120			α-ch	$(1)^4(2)^4(3)^4(4)^4(5)^4(6)^4(7)^4(8)^4$ $(9)^4$	107.70	[180,0,0]	α-ch[i]	[180,0,0]	(0,2.3)	10:1:1
^{44}Ti	0	3:3:2	(0,0.18)	GS(pro)	$[300]^4$	0.00	[32,20,20]	GS	[30,22,20]	(10.9,0.2)	1.2:1:1
	4		(38,0.52)					Tri$_4$	[34,28,14]	(43,0.4)	1.6:1.4:1
	12							SD(Pr)	[54,17,13]	(5.1,0.8)	2.2:1.1:1
	16		(0,0.86)	3:1[j]	$[200]^4[101]^4[110]^4[300]^4[210]^4$ $[201]^4[400]^4$	35.10	[64,12,12]	Pr$_{16}$	[63,13,12]	(1,1)	2.5:1:1
	24			2D(4:3)	$(1)^{-4}[20]^4[11]^4[02]^4[30]^4[21]^4[12]^4$ $[03]^4[31]^4$	95.49	[52,44,0]	Ob$_{24}$	[50,46,0]	(55.9,0.9)	3.3:3.1:1
	24		(60,1.5)					HD(Pr)	[75,12,9]	(2.3,1.2)	3.1:1.1:1
	28			2D(4:3)[k]	$(1)^{-4}[20]^4[11]^4[02]^4[30]^4[21]^4[12]^4$ $[40]^4[31]^4$ $[40]^4[31]^4$	92.89	[68,32,0]	Tri$_{28}$	[66,20,14]	(6.1,0.9)	2.4:1.2:1
	36							HD(Pr)	[80,17,11]	(4.5,1.2)	3.1:1.2:1
	48			2D(5:2)	$(1)^{-4}[20]^4[11]^4[21]^4[30]^4[40]^4[31]^4$ $[50]^4[41]^4$	103.04	[100,20,0]	EP$_{48}$	[105,9,6]	(1.5,1.6)	4.5:1.1:1

by introducing the so-called *reciprocal forbiddenness* with the following definition [34]:

$$S=\frac{1}{1+\min\sqrt{(\Delta n_1)^2+(\Delta n_2)^2+(\Delta n_3)^2}}. \tag{7}$$

Here $\Delta n_i=|n_i-n^c_{i,k}|$, where n_i stands for the U(3) *irrep* of the parent nucleus and $n^c_{i,k}$ refers to the U(3) *irrep* of the channel—the index k distinguishes the different product representations obtained from the right-hand side of Eq. (6). Based on this formula, the values $S\approx 0$ and $S\approx 1$ imply completely forbidden and completely allowed cluster

TABLE I. (*Continued.*)

		Energy surface		Bloch-Brink α-cluster model				SCS method			
Nucl.	$\hbar\omega$	$\omega_{x:y:z}$	(γ,ϵ)	α-conf.	Shell conf.	E	U(3)	Shape	$\mathrm{U(3)_{eff}}$	(γ,ϵ)	$a:b:c$
	52							EP_{52}	[106,11,7]	(2,1.6)	4.4:1.1:1
	84							EP_{84}	[148,6,2]	(1.4,2)	7.1:1.2:1
	148			α-ch	$(1)^4(2)^4(3)^4(4)^4(5)^4(6)^4(7)^4(8)^4$ $(9)^4(10)^4$	124.40	[220,0,0]	α-ch[l]	[220,0,0]	(0,2.3)	11:1:1

[a] This configuration is similar to the bipyramid one, but the α clusters on the symmetry axis are not equally separated from the center of mass of the three other clusters; four of the clusters in fact from an ^{16}O structure [11].

[b] According to the authors of Ref. [10], these two configurations are probably not orthogonal, since they share the configuration and very similar energies.

[c] The state $S(2:1)$ has an ^{16}O-^{16}O structure and corresponds to a pure deformed harmonic oscillator state [11].

[d] The authors of Ref. [10] found another shape isomer with the same shell configuration of slightly different energy, 64.57 MeV. Nevertheless, they did not specify the difference between these two configurations, but both of them can be assigned to be a 4p4h excitation of the state with $\omega_y:\omega_x=4:1$.

[e] Though this nucleus has a spherical shell-model ground state [11].

[f] It has an ^{16}O-^{8}Be-^{16}O structure [11].

[g] The authors of [10] observed three other shape isomers having the same shell configuration but of different energies (95.71, 96.24, and 96.66 MeV). They were thought to be the same physical state, since they have nearly equal binding energies and more or less the same shape, and more importantly they have the same shell-model limit.

[h] The authors of Ref. [10] discovered another shape isomer having the same shell configuration but of different energy, 95.33 MeV.

[i] Due to technical limitation of our program, this state was found by a manual calculation.

[j] This state is part of a family which starts with the $\alpha-\alpha-\alpha$ chain state in ^{12}C and extends up to ^{48}Cr [11]. Indeed, it has $^{16}\mathrm{O}-^{12}\mathrm{C}-^{16}\mathrm{O}$ structure.

[k] The authors of [10] found also a shape isomer with the same shell configuration of binding energy 93.49 MeV. Though they did not specify the difference between these two configurations, both of them can be interpreted as a 4p4h excitation of the state with $\omega_y:\omega_x=4:3$ or $\omega_y:\omega_x=5:2$; the geometries support the former one.

[l] Due to technical limitation of our program, this state was found by a manual calculation.

configurations, respectively. The results are displayed in Figs. 4 and 5. Note that there are several shape isomers and each may have more than one candidate because of the uncertainty of the effective quantum numbers, thus we manifest all possibilities for merely ^{12}C, ^{16}O, ^{20}Ne. Regarding to heavier nuclei, in addition to all shapes derived by the Bloch-Brink α-cluster model [9–11], only those from the SCS calculation that show strong agreement with the α-cluster model and can be expressed by a simple shell configuration are displayed.

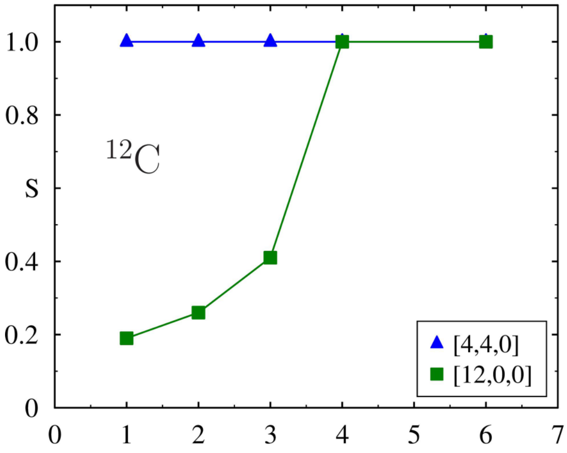

FIG. 4. Reciprocal forbiddenness as a function of the mass number of the lighter cluster for the different shape isomers of ^{12}C. The colored lines are just to guide the eye. Here, the continuous lines of different colors represent different shape isomers.

The $\mathrm{U^{ST}(4)}$ selection rule, unlike its U(3) counterpart, deals with spin-isospin symmetry and does not subsume the term belonging to the relative motion; it assumes

$$[f_1,f_2,f_3,f_4]=\left[f_1^A,f_2^A,f_3^A,f_4^A\right]\otimes\left[f_1^B,f_2^B,f_3^B,f_4^B\right], \quad (8)$$

where the left-hand side is the U(4) symmetry of the parent nucleus, while the right-hand side subsumes the U(4) symmetries of the two clusters.

A summary—containing all completely allowed binary cluster configurations for all candidates of every shape isomer—is tabulated in Table II.

V. CLUSTER-SHELL COEXISTENCE

The shell model and the cluster model are based on different physical pictures; thus, when we visualize these states naively, they are very different. In a phenomenological approach, they have orthogonal wave functions. The effect of the antisymmetrization, however, washes out somewhat the drastic difference between the models. As a result, the shell and cluster states may have finite overlap. This overlap can be considerable, sometimes even 100%. The same is the case with different cluster configurations.

As mentioned above, the U(3) symmetry was found as the common overlap between the shell and cluster models as early as 1958, wherefore the U(3) basis states can be a pure

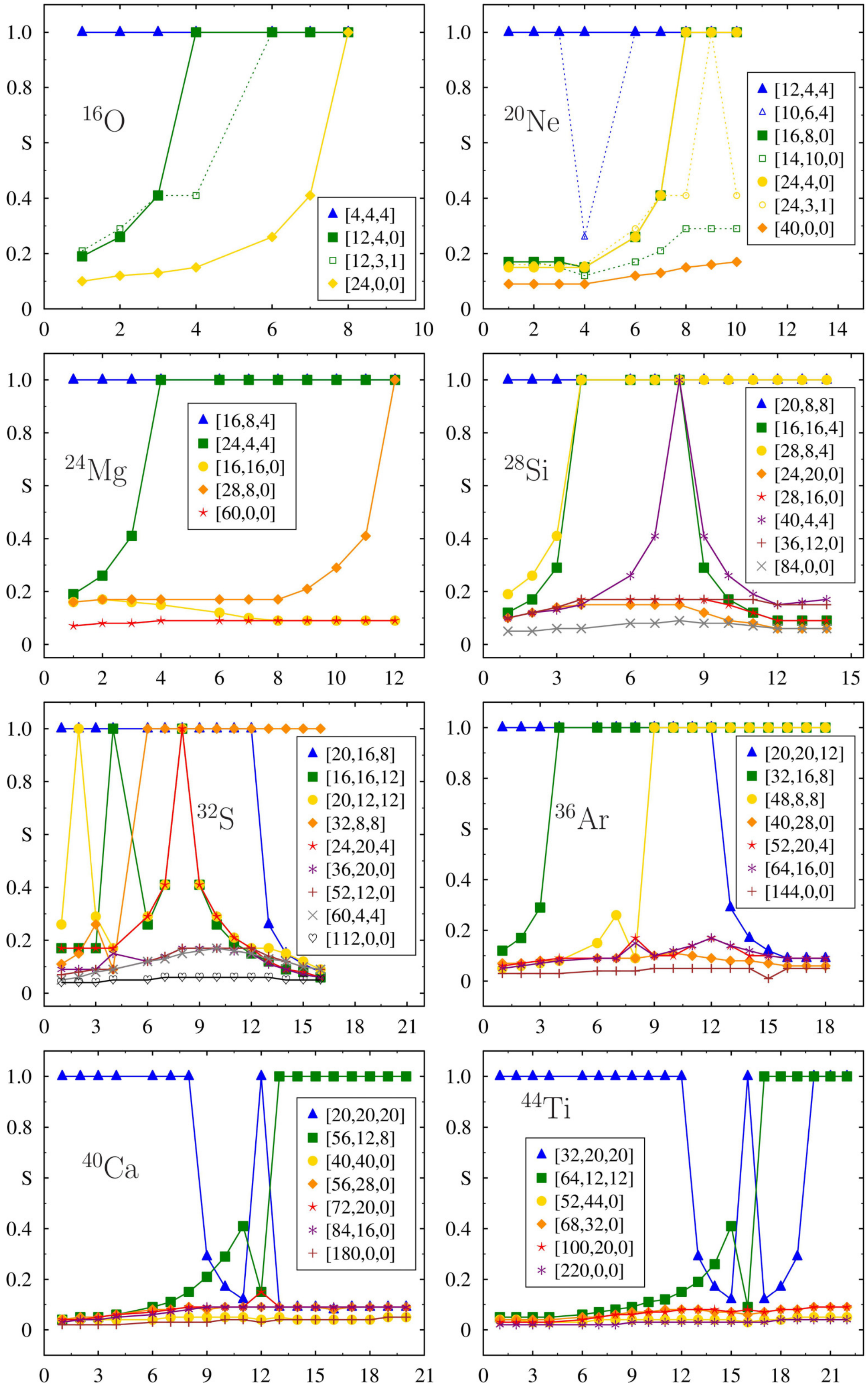

FIG. 5. Analogous to Fig. 4 for ^{16}O, ^{20}Ne, ^{24}Mg, ^{28}Si, ^{32}S, ^{36}Ar, ^{40}Ca, ^{44}Ti. Here the dotted lines indicate other candidates (effective symmetry) for the same shape isomer which is displayed by the continuous line of the same color.

TABLE II. Application of the U(3) and U$^{\mathrm{ST}}$(4) selection rules to determine possible binary clusterizations for different states of 4N-nuclei obtained from the SCS calculation and from the α-cluster (BB) model. The states are represented by U(3) quantum numbers. Those which are in italic format were achieved only from the BB model. The investigation was carried out only for stable isotopes in addition to ^{8}Be for systematic reason. Note that in this table, only completely allowed configurations are demonstrated, i.e., the reciprocal forbiddenness $S = 1$.

Nucl.	State	Possible clusterizations
^{12}C	[4,4,0]	^{1}H + ^{11}B, ^{2}H + ^{10}B, ^{3}He + ^{9}Be, ^{4}He + ^{8}Be, ^{6}Li + ^{6}Li
	[12,0,0]	^{4}He + ^{8}Be, ^{6}Li + ^{6}Li
^{16}O	[4,4,4]	^{1}H + ^{15}N, ^{2}H + ^{14}N, ^{3}He + ^{13}C, ^{4}He + ^{12}C, ^{6}Li + ^{10}B, ^{7}Li + ^{9}Be, ^{8}Be + ^{8}Be
	[12,4,0]	^{4}He + ^{12}C, ^{6}Li + ^{10}B, ^{7}Li + ^{9}Be, ^{8}Be + ^{8}Be
	[12,3,1]	^{6}Li + ^{10}B, ^{7}Li + ^{9}Be, ^{8}Be + ^{8}Be
	[24,0,0]	^{8}Be + ^{8}Be
^{20}Ne	[12,4,4]	^{1}H + ^{19}F, ^{2}H + ^{18}O, ^{3}He + ^{17}O, ^{4}He + ^{16}O, ^{6}Li + ^{14}N, ^{7}Li + ^{13}C, ^{8}Be + ^{12}C, ^{9}Be + ^{11}B, ^{10}B + ^{10}B
	[10,6,4]	^{1}H + ^{19}F, ^{2}H + ^{18}O, ^{3}He + ^{17}O, ^{6}Li + ^{14}N, ^{7}Li + ^{13}C, ^{8}Be + ^{12}C, ^{9}Be + ^{11}B, ^{10}B + ^{10}B
	[16,8,0]	^{8}Be + ^{12}C, ^{9}Be + ^{11}B, ^{10}B + ^{10}B
	[24,4,0]	^{8}Be + ^{12}C, ^{9}Be + ^{11}B, ^{10}B + ^{10}B
	[24,3,1]	^{9}Be + ^{11}B
^{24}Mg	*[16,8,4]*	^{1}H + ^{23}Na, ^{2}H + ^{22}Ne, ^{3}He + ^{21}Ne, ^{4}He + ^{20}Ne, ^{6}Li + ^{18}O, ^{7}Li + ^{17}O, ^{8}Be + ^{16}O, ^{9}Be + ^{15}N, ^{10}B + ^{14}N, ^{11}B + ^{13}C, ^{12}C + ^{12}C
	[16,7,5]	^{1}H + ^{23}Na, ^{2}H + ^{22}Ne, ^{3}He + ^{21}Ne, ^{6}Li + ^{18}O, ^{7}Li + ^{17}O, ^{9}Be + ^{15}N, ^{10}B + ^{14}N, ^{11}B + ^{13}C, ^{12}C + ^{12}C
	[13,10,5]	^{3}He + ^{21}Ne
	[24,4,4]	^{4}He + ^{20}Ne, ^{6}Li + ^{18}O, ^{7}Li + ^{17}O, ^{8}Be + ^{16}O, ^{9}Be + ^{15}N, ^{10}B + ^{14}N, ^{11}B + ^{13}C, ^{12}C + ^{12}C
	[28,8,0]	^{12}C + ^{12}C
	[27,6,3]	^{9}Be + ^{15}N, ^{10}B + ^{14}N, ^{11}B + ^{13}C, ^{12}C + ^{12}C
^{28}Si	*[20,8,8]*	^{1}H + ^{27}Al, ^{2}H + ^{26}Mg, ^{3}He + ^{25}Mg, ^{4}He + ^{24}Mg, ^{6}Li + ^{22}Ne, ^{7}Li + ^{21}Ne, ^{8}Be + ^{20}Ne, ^{9}Be + ^{19}F, ^{10}B + ^{18}O, ^{11}B + ^{17}O, ^{12}C + ^{16}O, ^{13}C + ^{15}N, ^{14}N + ^{14}N
	[19,9,8]	^{1}H + ^{27}Al, ^{2}H + ^{26}Mg, ^{3}He + ^{25}Mg, ^{4}He + ^{24}Mg, ^{6}Li + ^{22}Ne, ^{7}Li + ^{21}Ne, ^{8}Be + ^{20}Ne, ^{9}Be + ^{19}F, ^{10}B + ^{18}O, ^{11}B + ^{17}O
	[16,16,4]	^{4}He + ^{24}Mg, ^{6}Li + ^{22}Ne, ^{7}Li + ^{21}Ne, ^{8}Be + ^{20}Ne
	[16,15,5]	^{4}He + ^{24}Mg, ^{6}Li + ^{22}Ne, ^{7}Li + ^{21}Ne, ^{8}Be + ^{20}Ne
	[28,8,4]	^{4}He + ^{24}Mg, ^{6}Li + ^{22}Ne, ^{7}Li + ^{21}Ne, ^{8}Be + ^{20}Ne, ^{9}Be + ^{19}F, ^{10}B + ^{18}O, ^{11}B + ^{17}O, ^{12}C + ^{16}O, ^{13}C + ^{15}N, ^{14}N + ^{14}N
	[27,8,5]	^{3}He + ^{25}Mg, ^{4}He + ^{24}Mg, ^{6}Li + ^{22}Ne, ^{7}Li + ^{21}Ne, ^{8}Be + ^{20}Ne, ^{9}Be + ^{19}F, ^{10}B + ^{18}O, ^{11}B + ^{17}O, ^{12}C + ^{16}O, ^{13}C + ^{15}N, ^{14}N + ^{14}N
	[26,11,7]	^{1}H + ^{27}Al, ^{2}H + ^{26}Mg, ^{3}He + ^{25}Mg, ^{4}He + ^{24}Mg, ^{6}Li + ^{22}Ne, ^{7}Li + ^{21}Ne, ^{8}Be + ^{20}Ne, ^{9}Be + ^{19}F, ^{10}B + ^{18}O,
	[40,4,4]	^{8}Be + ^{20}Ne
	[35,8,5]	^{3}He + ^{25}Mg, ^{4}He + ^{24}Mg, ^{6}Li + ^{22}Ne, ^{7}Li + ^{21}Ne, ^{8}Be + ^{20}Ne, ^{9}Be + ^{19}F, ^{10}B + ^{18}O, ^{11}B + ^{17}O, ^{12}C + ^{16}O, ^{13}C + ^{15}N, ^{14}N + ^{14}N
^{32}S	[16,16,12]	^{4}He + ^{28}Si, ^{8}Be + ^{24}Mg
	[20,16,8]	^{1}H + ^{31}P, ^{2}H + ^{30}Si, ^{3}He + ^{29}Si, ^{4}He + ^{28}Si, ^{6}Li + ^{26}Mg, ^{7}Li + ^{25}Mg, ^{8}Be + ^{24}Mg, ^{9}Be + ^{23}Na, ^{10}B + ^{22}Ne, ^{11}B + ^{21}Ne, ^{12}C + ^{20}Ne
	[19,14,11]	^{7}Li + ^{25}Mg, ^{8}Be + ^{24}Mg, ^{9}Be + ^{23}Na
	[20,12,12]	^{2}H + ^{30}Si, ^{8}Be + ^{24}Mg
	[32,8,8]	^{6}Li + ^{26}Mg, ^{7}Li + ^{25}Mg, ^{8}Be + ^{24}Mg, ^{9}Be + ^{23}Na, ^{10}B + ^{22}Ne, ^{11}B + ^{21}Ne, ^{12}C + ^{20}Ne, ^{13}C + ^{19}F, ^{14}N + ^{18}O, ^{15}N + ^{17}O, ^{16}O + ^{16}O
	[31,9,8]	^{6}Li + ^{26}Mg, ^{7}Li + ^{25}Mg, ^{8}Be + ^{24}Mg, ^{9}Be + ^{23}Na, ^{10}B + ^{22}Ne, ^{11}B + ^{21}Ne, ^{12}C + ^{20}Ne, ^{13}C + ^{19}F, ^{14}N + ^{18}O, ^{15}N + ^{17}O
	[24,20,4]	^{8}Be + ^{24}Mg
	[44,7,5]	^{9}Be + ^{23}Na, ^{10}B + ^{22}Ne, ^{11}B + ^{21}Ne
	[51,8,5]	^{7}Li + ^{25}Mg, ^{8}Be + ^{24}Mg, ^{9}Be + ^{23}Na, ^{10}B + ^{22}Ne, ^{11}B + ^{21}Ne, ^{12}C + ^{20}Ne, ^{13}C + ^{19}F
^{36}Ar	*[20,20,12]*	^{1}H + ^{35}Cl, ^{2}H + ^{34}S, ^{3}He + ^{33}S, ^{4}He + ^{32}S, ^{6}Li + ^{30}Si, ^{7}Li + ^{29}Si, ^{8}Be + ^{28}Si, ^{9}Be + ^{27}Al, ^{10}B + ^{26}Mg, ^{11}B + ^{25}Mg, ^{12}C + ^{24}Mg
	[20,19,13]	^{1}H + ^{35}Cl, ^{2}H + ^{34}S, ^{3}He + ^{33}S, ^{4}He + ^{32}S, ^{6}Li + ^{30}Si, ^{7}Li + ^{29}Si, ^{8}Be + ^{28}Si,
	[26,22,8]	^{6}Li + ^{30}Si, ^{7}Li + ^{29}Si, ^{9}Be + ^{27}Al, ^{10}B + ^{26}Mg

TABLE II. (*Continued.*)

Nucl.	State	Possible clusterizations
	[32,16,8]	^{4}He + ^{32}S, ^{6}Li + ^{30}Si, ^{7}Li + ^{29}Si, ^{8}Be + ^{28}Si, ^{9}Be + ^{27}Al, ^{10}B + ^{26}Mg, ^{11}B + ^{25}Mg, ^{12}C + ^{24}Mg, ^{13}C + ^{23}Na, ^{14}N + ^{22}Ne, ^{15}N + ^{21}Ne, ^{16}O + ^{20}Ne, ^{17}O + ^{19}F, ^{18}O + ^{18}O
	[30,15,11]	^{6}Li + ^{30}Si, ^{7}Li + ^{29}Si, ^{9}Be + ^{27}Al, ^{10}B + ^{26}Mg, ^{11}B + ^{25}Mg, ^{12}C + ^{24}Mg, ^{13}C + ^{23}Na
	[39,12,9]	^{6}Li + ^{30}Si, ^{7}Li + ^{29}Si, ^{9}Be + ^{27}Al, ^{10}B + ^{26}Mg, ^{11}B + ^{25}Mg, ^{12}C + ^{24}Mg, ^{13}C + ^{23}Na, ^{14}N + ^{22}Ne, ^{15}N + ^{21}Ne, ^{17}O + ^{19}F, ^{18}O + ^{18}O
	[48,8,8]	^{9}Be + ^{27}Al, ^{10}B + ^{26}Mg, ^{11}B + ^{25}Mg, ^{12}C + ^{24}Mg, ^{13}C + ^{23}Na, ^{14}N + ^{22}Ne, ^{15}N + ^{21}Ne, ^{16}O + ^{20}Ne, ^{17}O + ^{19}F, ^{18}O + ^{18}O
	[51,10,7]	^{9}Be + ^{27}Al, ^{10}B + ^{26}Mg, ^{11}B + ^{25}Mg, ^{12}C + ^{24}Mg, ^{13}C + ^{23}Na, ^{14}N + ^{22}Ne, ^{15}N + ^{21}Ne
^{40}Ca	[20,20,20]	^{1}H + ^{39}K, ^{2}H + ^{38}Ar, ^{3}He + ^{37}Cl, ^{4}He + ^{36}Ar, ^{4}He + ^{36}S, ^{6}Li + ^{34}S, ^{7}Li + ^{33}S, ^{8}Be + ^{32}S, ^{12}C + ^{28}Si
	[28,23,13]	^{7}Li + ^{33}S, ^{8}Be + ^{32}S, ^{9}Be + ^{31}P, ^{10}B + ^{30}Si, ^{11}B + ^{29}Si
	[38,17,13]	^{7}Li + ^{33}S, ^{8}Be + ^{32}S, ^{9}Be + ^{31}P, ^{10}B + ^{30}Si, ^{11}B + ^{29}Si, ^{12}C + ^{28}Si, ^{17}O + ^{23}Na, ^{18}O + ^{22}Ne, ^{19}F + ^{21}Ne, ^{20}Ne + ^{20}Ne
	[56,12,8]	^{13}C + ^{27}Al, ^{14}N + ^{26}Mg, ^{15}N + ^{25}Mg, ^{16}O + ^{24}Mg, ^{17}O + ^{23}Na, ^{18}O + ^{22}Ne, ^{19}F + ^{21}Ne, ^{20}Ne + ^{20}Ne
	[52,19,13]	^{6}Li + ^{34}S, ^{7}Li + ^{33}S, ^{8}Be + ^{32}S, ^{10}B + ^{30}Si, ^{11}B + ^{29}Si, ^{17}O + ^{23}Na, ^{18}O + ^{22}Ne, ^{19}F + ^{21}Ne, ^{20}Ne + ^{20}Ne
	[63,15,10]	^{9}Be + ^{31}P, ^{10}B + ^{30}Si, ^{11}B + ^{29}Si, ^{13}C + ^{27}Al, ^{14}N + ^{26}Mg, ^{15}N + ^{25}Mg, ^{16}O + ^{24}Mg, ^{17}O + ^{23}Na, ^{18}O + ^{22}Ne, ^{19}F + ^{21}Ne, ^{20}Ne + ^{20}Ne
^{44}Ti	*[32,20,20]*	^{1}H + ^{43}Ca, ^{2}H + ^{42}Ca, ^{3}He + ^{41}K, ^{4}He + ^{40}Ar, ^{4}He + ^{40}Ca, ^{4}He + ^{40}K, ^{6}Li + ^{38}Ar, ^{7}Li + ^{37}Cl, ^{8}Be + ^{36}Ar, ^{8}Be + ^{36}S, ^{9}Be + ^{35}Cl, ^{10}B + ^{34}S, ^{11}B + ^{33}S, ^{12}C + ^{32}S, ^{16}O + ^{28}Si, ^{20}Ne + ^{24}Mg, ^{21}Ne + ^{23}Na, ^{22}Ne + ^{22}Ne
	[30,22,20]	^{1}H + ^{43}Ca, ^{2}H + ^{42}Ca, ^{3}He + ^{41}K, ^{6}Li + ^{38}Ar, ^{7}Li + ^{37}Cl, ^{8}Be + ^{36}Ar, ^{8}Be + ^{36}S, ^{9}Be + ^{35}Cl, ^{10}B + ^{34}S, ^{11}B + ^{33}S, ^{12}C + ^{32}S
	[54,17,13]	^{11}B + ^{33}S, ^{12}C + ^{32}S, ^{13}C + ^{31}P, ^{14}N + ^{30}Si, ^{15}N + ^{29}Si, ^{17}O + ^{27}Al, ^{18}O + ^{26}Mg, ^{19}F + ^{25}Mg, ^{20}Ne + ^{24}Mg, ^{21}Ne + ^{23}Na, ^{22}Ne + ^{22}Ne
	[64,12,12]	^{17}O + ^{27}Al, ^{18}O + ^{26}Mg, ^{19}F + ^{25}Mg, ^{20}Ne + ^{24}Mg, ^{21}Ne + ^{23}Na, ^{22}Ne + ^{22}Ne
	[63,13,12]	^{22}Ne + ^{22}Ne
	[75,12,9]	^{19}F + ^{25}Mg, ^{20}Ne + ^{24}Mg, ^{21}Ne + ^{23}Na, ^{22}Ne + ^{22}Ne
	[66,20,14]	^{7}Li + ^{37}Cl, ^{8}Be + ^{36}Ar, ^{8}Be + ^{36}S, ^{9}Be + ^{35}Cl, ^{10}B + ^{34}S, ^{11}B + ^{33}S, ^{12}C + ^{32}S, ^{13}C + ^{31}P, ^{14}N + ^{30}Si, ^{15}N + ^{29}Si, ^{21}Ne + ^{23}Na, ^{17}O + ^{27}Al, ^{18}O + ^{26}Mg, ^{19}F + ^{25}Mg, ^{20}Ne + ^{24}Mg, ^{21}Ne + ^{23}Na, ^{22}Ne + ^{22}Ne
	[80,17,11]	^{12}C + ^{32}S, ^{13}C + ^{31}P, ^{14}N + ^{30}Si, ^{15}N + ^{29}Si, ^{17}O + ^{27}Al, ^{18}O + ^{26}Mg, ^{19}F + ^{25}Mg, ^{20}Ne + ^{24}Mg, ^{21}Ne + ^{23}Na, ^{22}Ne + ^{22}Ne

shell model and a pure cluster state at the same time. This situation happens when the multiplicity of the basis state is 1. In such a case, the cluster-model wave function can be written as a linear combination of a single term of the shell basis [of the relevant U(3) symmetry], i.e., they are identical. This phenomenon is well known for some ground (and low-lying) states of light nuclei for a long time.

It turns out that (i) stable U(3) symmetry characterizes several high-lying states, with large deformation, as well, which are known as the shape isomers. Furthermore, (ii) many of them have the same simple shell connection, as those found earlier in the ground-state region.

Here we investigate this question for the shape isomers, described in the previous sections. In particular, Table III lists those shell configurations which have single multiplicity, and their possible binary clusterizations in terms of α-like clusters. When a shape isomer has more than one candidate for the U(3) symmetry, we take the one which corresponds to a simple shell configuration, which usually coincides with the ones obtained from the α-cluster calculations. Figure 6 shows the shell and cluster configurations with wave functions of 100% overlap.

VI. ENERGY SPECTRA

A. The energy functional

In MUSY-based studies, one usually applies a simple dynamically symmetric Hamiltonian. In spite of its simplicity, however, it seems to be able to describe the gross features of the spectra, including spectra of the ground-state region, as well as those of the superdeformed and hyperdeformed minima [13]. It is expressed in terms of the invariant operators of the group-chain: U(3) $\supset$ SU(3) $\supset$ SO(3) basis [14]:

$$\mathbf{H} = (\hbar\omega)\mathbf{n} + a\mathbf{C}^{(\mathbf{2})}_{\mathbf{SU(3)}} + b\mathbf{C}^{(\mathbf{3})}_{\mathbf{SU(3)}} + d\frac{1}{2\theta}\mathbf{L}^2, \qquad (9)$$

where the first constituent is the harmonic oscillator Hamiltonian, the second one possessing the eigenvalue $\lambda^2 + \mu^2 + \lambda\mu + 3(\lambda + \mu)$ stems from the quadrupole-quadrupole interaction, the third operator with the expected value $(\lambda - \mu)(\lambda + 2\mu + 3)(2\lambda + \mu + 3)$ splits the degeneracy of the prolate and oblate shapes, and the last one is related to the three-dimensional rotation. This Hamiltonian is symmetric with respect to transformations between the different configurations [5].

TABLE III. Shell-model multiplicity 1 representations with possible α-like clusterizations from the BB-model and SCS calculations. The ones in italic format are from the BB model, but very close correspondent was found in SCS, too.

Nucl.	$\hbar\omega$	State	Possible α-like clusterizations
^{12}C	0	[4,4,0]	^{4}He + ^{8}Be
	4	[12,0,0]	^{4}He + ^{8}Be
^{16}O	0	[4,4,4]	^{4}He + ^{12}C, ^{8}Be + ^{8}Be
	4	*[12,4,0]*	^{4}He + ^{12}C, ^{8}Be + ^{8}Be
	12	[24,0,0]	^{8}Be + ^{8}Be
^{20}Ne	0	[12,4,4]	^{4}He + ^{16}O, ^{8}Be + ^{12}C
	0	[10,6,4]	^{8}Be + ^{12}C
	4	[14,10,0]	
	4	*[16,8,0]*	^{8}Be + ^{12}C
	8	*[24,4,0]*	^{8}Be + ^{12}C
	20	[40,0,0]	
^{24}Mg	0	*[16,8,4]*	^{4}He + ^{20}Ne, ^{8}Be + ^{16}O, ^{12}C + ^{12}C
	0	[13,10,5]	
	4	[24,4,4]	^{4}He + ^{20}Ne, ^{8}Be + ^{16}O, ^{12}C + ^{12}C
	4	[16,16,0]	
	8	*[28,8,0]*	^{12}C + ^{12}C
	32	[60,0,0]	
^{28}Si	0	*[20,8,8]*	^{4}He + ^{24}Mg, ^{8}Be + ^{20}Ne, ^{12}C + ^{16}O
	0	[14,13,9]	
	0	*[16,16,4]*	^{4}He + ^{24}Mg, ^{8}Be + ^{20}Ne
	4	*[28,8,4]*	^{4}He + ^{24}Mg, ^{8}Be + ^{20}Ne, ^{12}C + ^{16}O,
	8	[24,20,0]	
	8	*[28,16,0]*	
	12	[40,4,4]	^{8}Be + ^{20}Ne
	48	[84,0,0]	
^{32}S	0	[19,14,11]	^{8}Be + ^{24}Mg
	0	*[20,16,8]*	^{4}He + ^{28}Si, ^{8}Be + ^{24}Mg, ^{12}C + ^{20}Ne
	0	*[20,12,12]*	^{8}Be + ^{24}Mg
	4	[31,9,8]	^{8}Be + ^{24}Mg, ^{12}C + ^{20}Ne
	4	*[32,8,8]*	^{8}Be + ^{24}Mg, ^{12}C + ^{20}Ne, ^{16}O + ^{16}O
	4	[24,20,4]	^{8}Be + ^{24}Mg
	12	[36,20,0]	
	20	*[52,12,0]*	
	24	[60,4,4]	
	68	[112,0,0]	
^{36}Ar	0	*[20,20,12]*	^{4}He + ^{32}S, ^{8}Be + ^{28}Si, ^{12}C + ^{24}Mg
	4	*[32,16,8]*	^{4}He + ^{32}S, ^{8}Be + ^{28}Si, ^{12}C + ^{24}Mg, ^{16}O + ^{20}Ne
	12	[48,8,8]	^{12}C + ^{24}Mg, ^{16}O + ^{20}Ne
	16	*[40,28,0]*	
	20	*[52,20,0]*	
	92	[144,0,0]	
^{40}Ca	0	[20,20,20]	^{4}He + ^{36}Ar, ^{8}Be + ^{32}S, ^{12}C + ^{28}Si
	16	[56,12,8]	^{16}O + ^{24}Mg, ^{20}Ne + ^{20}Ne
	20	*[40,40,0]*	
	24	*[56,28,0]*	
	32	*[72,20,0]*	
	120	[180,0,0]	
^{44}Ti	0	*[32,20,20]*	^{4}He + ^{40}Ca, ^{8}Be + ^{36}Ar, ^{12}C + ^{32}S, ^{16}O + ^{28}Si, ^{20}Ne + ^{24}Mg
	0	[30,22,20]	^{8}Be + ^{36}Ar, ^{12}C + ^{32}S
	16	*[64,12,12]*	^{20}Ne + ^{24}Mg
	28	*[68,32,0]*	
	148	[220,0,0]	

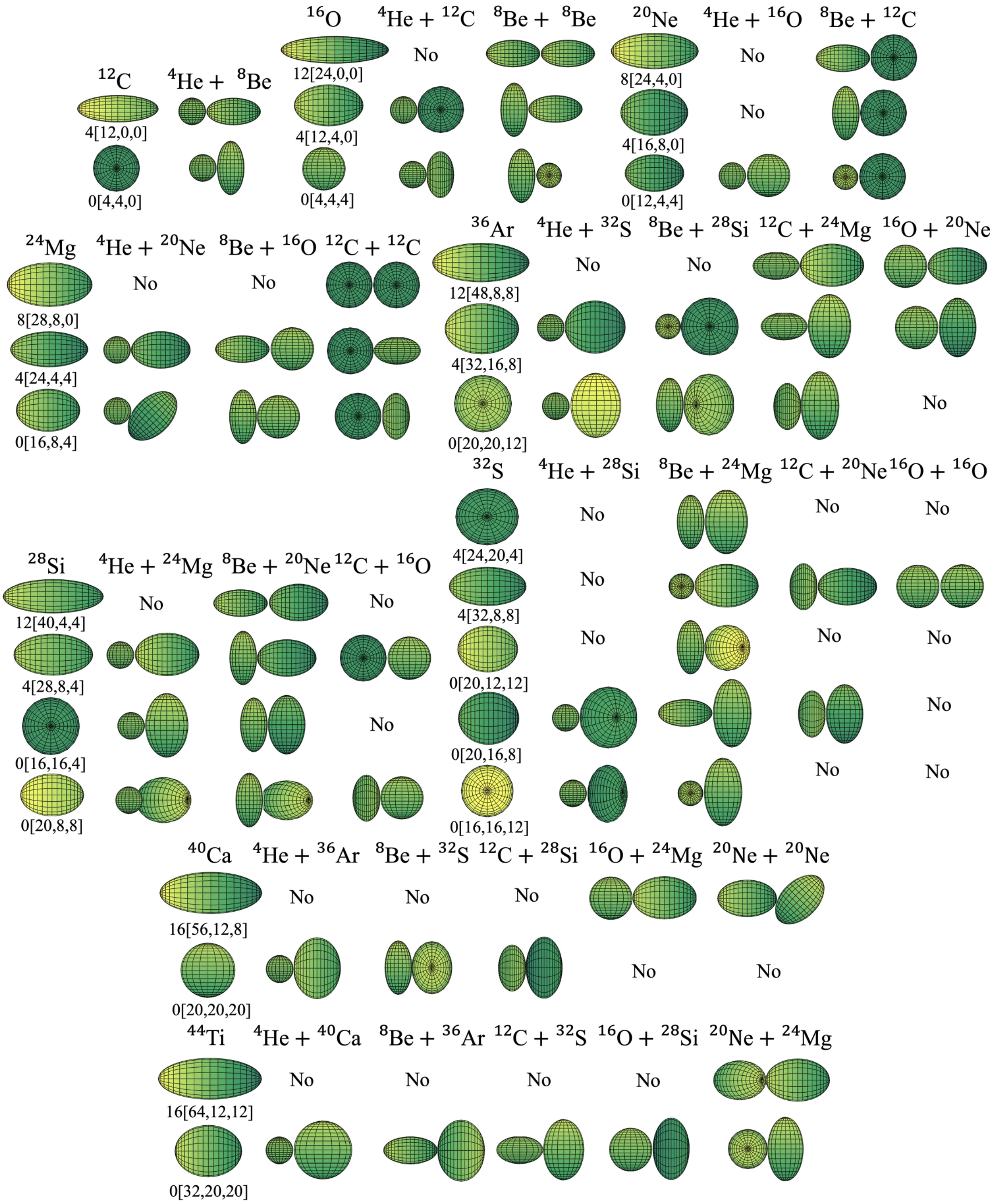

FIG. 6. Some shape isomers (with simple shell configurations) of ^{12}C, ^{16}O, ^{20}Ne, ^{24}Mg, ^{28}Si, ^{32}S, ^{36}Ar, ^{40}Ca, ^{44}Ti are juxtaposed with their corresponding binary α-like cluster configurations which show 100% overlap with the shell-model wave functions. In front of the square brackets is the major shell excitation quanta, whereas the U(3) symmetry of the shape is indicated inside the square brackets. The clusters were drawn in such a way that the z and x axes are in the plane of the paper and are horizontal and vertical, respectively; meanwhile, the y axis is perpendicular to the plane of the paper.

Here we apply this Hamiltonian for the description of the energy spectra of the shape isomers of 4N nuclei. Since we know only the ground-state band head in each local minimum, the last term of the Hamiltonian is irrelevant in the present case, i.e.,

$$\mathbf{H} = (\hbar\omega)\mathbf{n} + a\mathbf{C}^{(2)}_{\mathbf{SU(3)}} + b\mathbf{C}^{(3)}_{\mathbf{SU(3)}}. \qquad (10)$$

B. Result

The investigation is carried out using the results of the BB model [9–11], which were summarized in Table I. To be specific, we try to determine $\hbar\omega$, a, b in Eq. (10) in such a way that the deviation from the BB energy is the smallest.

In Eq. (10) lie three parameters, thus nuclei equipped with less than three configurations, namely ^{8}Be and ^{12}C, cannot be considered.

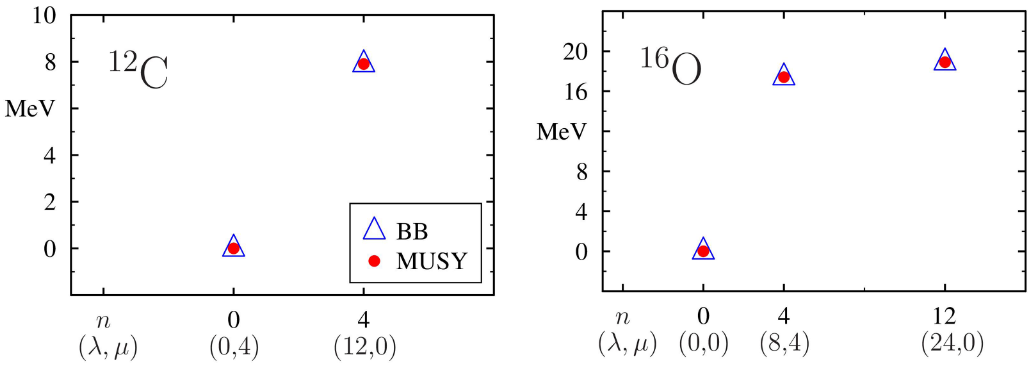

FIG. 7. The energy spectra of ^{12}C and ^{16}O calculated by the simple MUSY Hamiltonian $\mathbf{H} = (\hbar\omega)\mathbf{n} + a\mathbf{C}^{(2)}_{\mathbf{SU(3)}}$ in comparison with that determined by the α-cluster (BB) model.

In Refs. [9–11], for some heavy nuclei, including

$$^{48}\mathrm{Cr},\ ^{52}\mathrm{Fe},\ ^{56}\mathrm{Ni},\ ^{60}\mathrm{Zn},$$

the authors calculated only the energy of the linear α-chain state, thus the whole spectrum cannot be described.

For the rest of the nuclei, the regression is carried out utilizing the well-known least square method, in which we minimize the function

$$F = \sum_{i=1}^{m} \left(E_i^{\mathrm{MUSY}} - E_i^{\mathrm{BB}}\right)^2, \tag{11}$$

where m is the total number of states to be fitted, E_i^{MUSY} and E_i^{BB} are energies calculated based on the two models—MUSY and BB—respectively.

We have tested also the performance of an even simpler Hamiltonian with $b = 0$, whereby ^{12}C can be examined as well. That is, Eq. (10) reduces to

$$\mathbf{H} = (\hbar\omega)\mathbf{n} + a\mathbf{C}^{(2)}_{\mathbf{SU(3)}}. \tag{12}$$

Please note that for the ^{16}O case one can apply only the two-parameter functional, too. It has three shape isomers, but due to the special quantum numbers of its ground state ($n = \lambda = \mu = 0$), there are only two equations, so the three-parameter problem is undefined. The results of both investigations are presented in in Figs. 7–9, and the parameters are shown in Table IV, and Fig. 10.

It is blatant that almost every nucleus is governed by the model in case of three terms in Eq. (10) (except for ^{28}Si, which has slightly larger deviation—acceptable notwithstanding). The exclusion of the last element results in larger deviation, of course, but still showing considerable similarities between the spectra of the two models.

VII. SUMMARY AND CONCLUSIONS

In this work, we investigated the shape isomers of $N = Z$ nuclei by applying the multiconfigurational dynamical symmetry. The shape isomers were obtained from a study of the stability and self-consistency of the U(3) symmetry. This is the connecting symmetry of the shell, collective, and cluster models not only for a single-shell problem, as uncovered in 1958, but also for the multishell excitations, where it appears as the united symmetry of the valance shell (or internal cluster) $\mathrm{U}_s(3)$ group and the $\mathrm{U}_e(3)$ excitation group, $\mathrm{U}_s(3) \otimes \mathrm{U}_e(3) \supset \mathrm{U}(3)$. It determines uniquely the quadrupole shape, thus the stability and self-consistency of the shape was investigated. The real U(3) is not general enough to be valid in a large range of deformation and energy, therefore, the quasidynamical symmetry was applied, which coincides with the real one when the latter is valid. Nilsson

TABLE IV. Results of the determination of the parameters (in MeV) of the MUSY Hamiltonian. The error of the calculation is determined by the formula $\mathrm{Err}^2 = \frac{\mathrm{F}}{\mathrm{m}} = \frac{1}{\mathrm{m}}\sum_{\mathrm{i}=1}^{\mathrm{m}}(\mathrm{H}_\mathrm{i}^{\mathrm{MUSY}} - \mathrm{H}_\mathrm{i}^{\mathrm{BB}})^2$, where m is the total number of states to be fitted. The closer the error to zero, the more compatible the MUSY-based energy is with the energy produced in the α-cluster model.

	$\mathbf{H} = (\hbar\omega)\mathbf{n} + a\mathbf{C}^{(2)}_{\mathbf{SU(3)}} + b\mathbf{C}^{(3)}_{\mathbf{SU(3)}}$				$\mathbf{H} = (\hbar\omega)\mathbf{n} + a\mathbf{C}^{(2)}_{\mathbf{SU(3)}}$		
Nucl.	$\hbar\omega$	a	b	Err	$\hbar\omega$	a	Err
^{12}C					5.000	−0.07961	0.000
^{16}O					10.398	−0.16338	0.000
^{20}Ne	9.682	−0.120	0.00024	0.716	7.706	−0.07509	0.819
^{24}Mg	17.093	−0.221	0.00065	1.569	7.968	−0.05783	3.059
^{28}Si	6.902	−0.048	0.00005	3.744	5.702	−0.03004	3.835
^{32}S	8.180	−0.060	0.00010	1.911	4.325	−0.01725	3.808
^{36}Ar	9.781	−0.067	0.00010	2.660	4.954	−0.01734	5.760
^{40}Ca	10.692	−0.063	0.00008	2.901	5.788	−0.01793	10.383
^{44}Ti	8.888	−0.045	0.00005	0.831	4.485	−0.01107	9.550

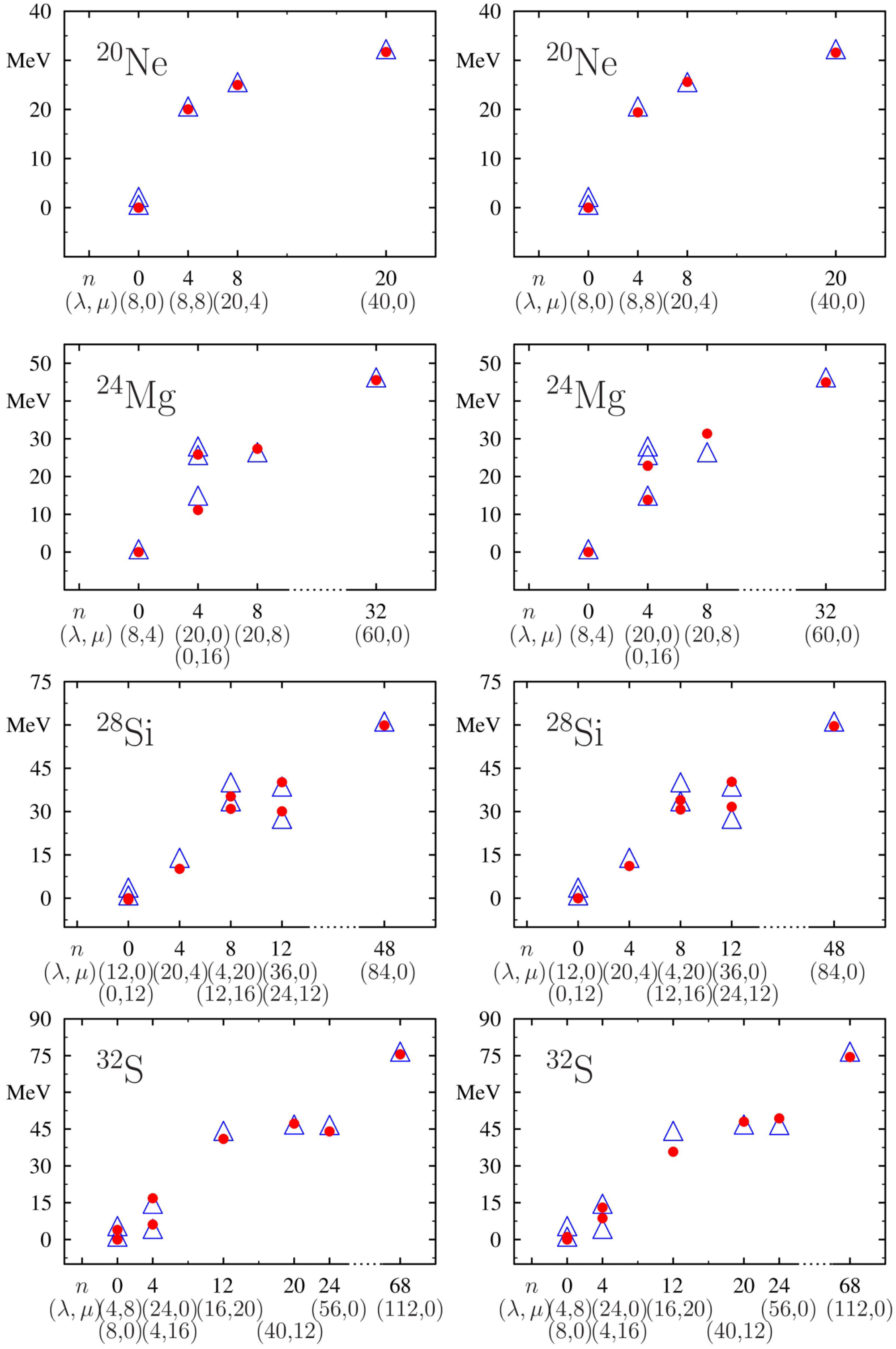

FIG. 8. The energy spectrum of ^{16}O, ^{20}Ne, ^{24}Mg, ^{28}Si, ^{32}S calculated by the two simple MUSY Hamiltonians (dots) in comparison with that determined by the α-cluster (BB) model (triangles). The figures on the left-hand side correspond to $\mathbf{H} = (\hbar\omega)\mathbf{n} + a\mathbf{C}^{(2)}_{\mathbf{SU(3)}} + b\mathbf{C}^{(3)}_{\mathbf{SU(3)}}$, while those on the right-hand side correspond to $\mathbf{H} = (\hbar\omega)\mathbf{n} + a\mathbf{C}^{(2)}_{\mathbf{SU(3)}}$.

calculations were performed, and the shape isomers appeared as plateaus of the physical β parameter as a function of the input deformation.

Several shape isomers emerged for nuclei ranging from ^{12}C to ^{44}Ti. The results show remarkable similarity to the previous ones from energy-minimum calculations of the Nilsson model, and very good agreement with those of the Bloch-Brink α-cluster model. (The α-model and our SCS method give more shape isomers than the Nilsson energy surfaces.)

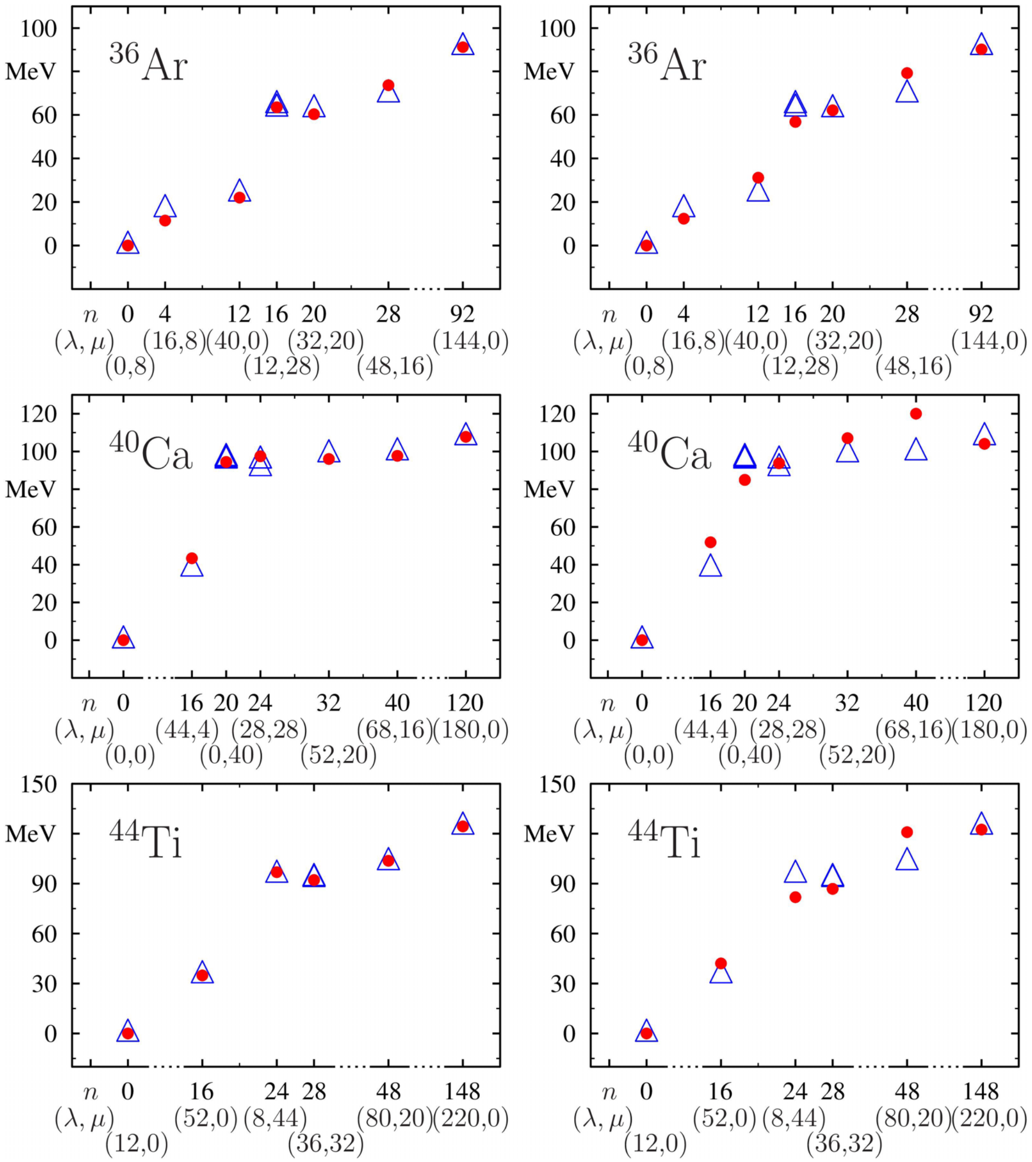

FIG. 9. Analogous to Fig. 8 for ^{36}Ar, ^{40}Ca, and ^{44}Ti.

Based on the U(3) and spin-isospin $\mathrm{U}^{\mathrm{ST}}(4)$ selection rules, the allowed binary cluster configurations of the shape isomers were determined. This is only a necessary condition, of course, the energetic aspects of the problem were not considered. Nevertheless, it can be an useful piece of information even from the experimental viewpoint, in light of the fact that the cluster configuration and the reaction channels are uniquely related to each other.

A major point of the present work is the investigation of the energy distribution of the shape isomers. Beforehand MUSY was applied for the unified description of the spectra in the first, second, and third valleys, that is to say, it was used in the ground, superdeformed and hyperdeformed minima. A very remarkable founding was that a very simple energy-functional with only three parameters could reproduce the experimental spectrum in a large range of excitation energy and quadrupole deformation. Here we addressed the question whether the simple dynamically symmetric Hamiltonian is able to produce realistic energies for the complete spectra of shape isomers. Due to the fact that the available experimental data are rather limited, we tried to reproduce the energy spectra, which were obtained from the BB α-cluster model. It turns out that the energy of all the shape isomers can be obtained with a good approximation with a very simple energy functional, containing only three parameters: the oscillator energy, the quadrupole force, and a deformation-dependent part that makes difference between the prolate and oblate shapes. Furthermore, even the first two terms gave a remarkable concurrence. In this calculation only a single state, "the ground state," was calculated in each valley, since only the local minima are available from the α-cluster model. It is worth emphasizing, however, that MUSY allows the determination of the detailed spectra as well, and not only for a shell or quartet configuration, but for different clusterizations, as well.

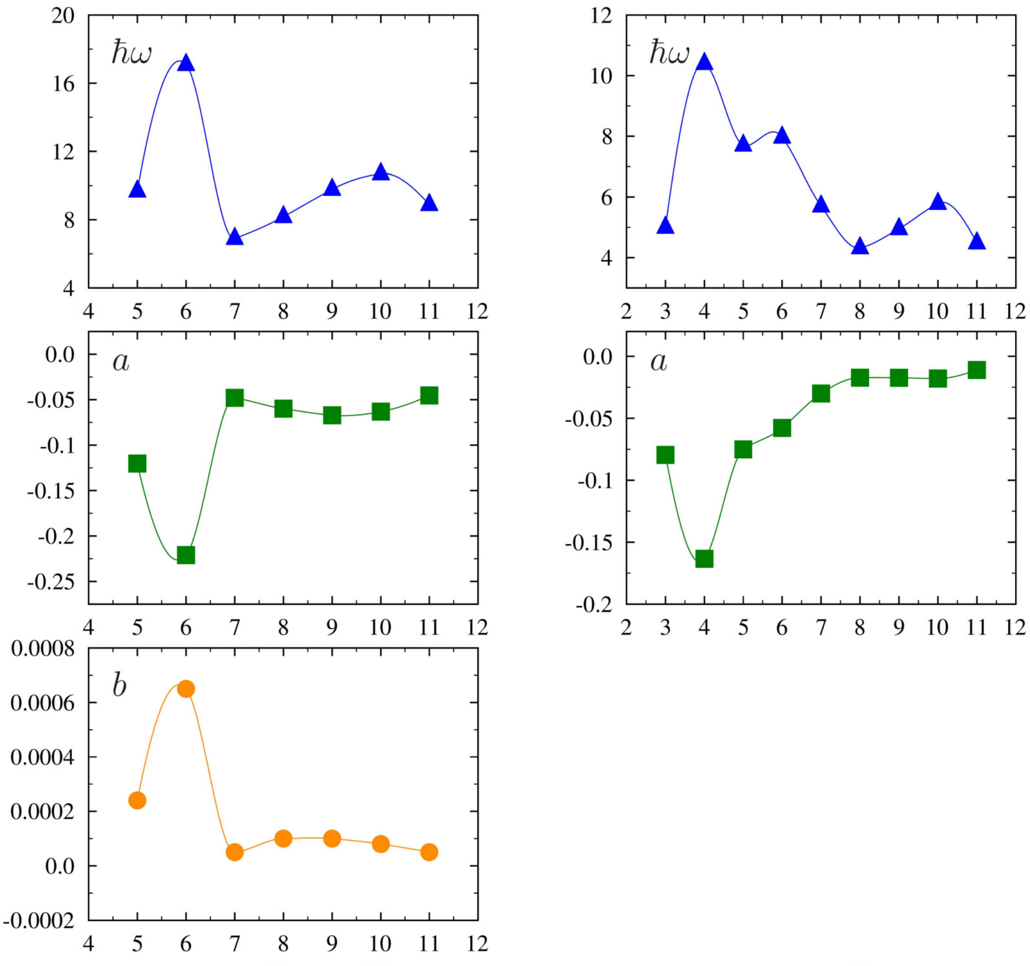

(a) $\mathbf{H} = (\hbar\omega)\mathbf{n} + a\mathbf{C}^{(\mathbf{2})}_{\mathbf{SU(3)}} + b\mathbf{C}^{(\mathbf{3})}_{\mathbf{SU(3)}}$

(b) $\mathbf{H} = (\hbar\omega)\mathbf{n} + a\mathbf{C}^{(\mathbf{2})}_{\mathbf{SU(3)}}$

FIG. 10. Fitted values of $\hbar\omega$, a, b (MeV) as functions of $N = A/4$ for the two simple MUSY Hamiltonians.

ACKNOWLEDGMENTS

This work was supported by the National Research, Development and Innovation Fund of Hungary, financed under the K18 funding scheme with Project No. K 128729. In addition, financial support from TalentUD program of the University of Debrecen, Hungary, is appreciated.

---

[1] C. W. Johnson, Spin-orbit decomposition of ab initio nuclear wave functions, Phys. Rev. C **91**, 034313 (2015).

[2] J. Johnson, Shadows of symmetries, Nucl. Phys. News **29**, 18 (2019).

[3] T. Dytrych, K. D. Launey, J. P. Draayer, D. J. Rowe, J. L. Wood, G. Rosensteel, C. Bahri, D. Langr, and R. B. Baker, Physics of Nuclei: Key Role of an Emergent Symmetry, Phys. Rev. Lett. **124**, 042501 (2020).

[4] K. Launey, T. Dytrych, G. Sargsyan, R. Baker, and J. Draayer, Emergent symplectic symmetry in atomic nuclei, Eur. Phys. J. Spec. Top. **229**, 2429 (2020).

[5] J. Cseh, Microscopic structure and mathematical background of the multiconfigurational dynamical symmetry, Phys. Rev. C **103**, 064322 (2021).

[6] J. Cseh, G. Riczu, and J. Darai, A symmetry in-between the shapes, shells, and clusters of nuclei, Symmetry **15**, 115 (2023).

[7] J. Draayer, *Algebraic Approaches to Nuclear Structure*, edited by R. F. Casten (Academic Press, New York, 1993), p. 423.

[8] J. Cseh, G. Riczu, and J. Darai, Shape isomers of light nuclei from the stability and consistency of the SU(3) symmetry, Phys. Lett. B **795**, 160 (2019).

[9] A. Merchant and W. Rae, Systematics of alpha-chain states in 4N-nuclei, Nucl. Phys. A **549**, 431 (1992).

[10] J. Zhang and W. Rae, Systematics of 2-dimensional α-cluster configurations in 4N nuclei from ^{12}C to ^{44}Ti, Nucl. Phys. A **564**, 252 (1993).

[11] J. Zhang, W. Rae, and A. Merchant, Systematics of some 3-dimensional α-cluster configurations in 4N nuclei from ^{16}O to ^{44}Ti, Nucl. Phys. A **575**, 61 (1994).

[12] G. Leander and S. Larsson, Potential-energy surfaces for the doubly even $N = Z$ nuclei, Nucl. Phys. A **239**, 93 (1975).

[13] G. Riczu and J. Cseh, Gross features of the spectrum of the ^{36}Ar nucleus, Int. J. Mod. Phys. E **30**, 2150034 (2021).

[14] J. Cseh and G. Riczu, Quartet excitations and cluster spectra in light nuclei, Phys. Lett. B **757**, 312 (2016).

[15] G. Riczu and J. Cseh, A unified description of spectra of different configurations, deformation and energy regions, Bulg. J. Phys. **48**, 524 (2021).

[16] P. Adsley, D. G. Jenkins, J. Cseh, S. S. Dimitriova, J. W. Brummer, K. C. W. Li, D. J. Marin-Lambarri, K. Lukyanov, N. Y. Kheswa, R. Neveling, P. Papka, L. Pellegri, V. Pesudo, L. C. Pool, G. Riczu, F. D. Smit, J. J. van Zyl, and E. Zemlyanaya, Alpha clustering in ^{28}Si probed through the identification of high-lying 0^+ states, Phys. Rev. C **95**, 024319 (2017).

[17] J. Elliott, Collective motion in the nuclear shell model. I. Classification schemes for states of mixed configurations, Proc. Roy. Soc. A **245**, 128 (1958).

[18] K. Wildermuth and T. Kanellopoulos, The "cluster model" of the atomic nuclei, Nucl. Phys. **7**, 150 (1958).

[19] B. Bayman and A. Bohr, On the connection between the cluster model and the SU(3) coupling scheme for particles in a harmonic oscillator potential, Nucl. Phys. **9**, 596 (1958).

[20] G. Rosensteel and D. Rowe, Nuclear Sp(3, R) Model, Phys. Rev. Lett. **38**, 10 (1977).

[21] G. Rosensteel and D. Rowe, On the algebraic formulation of collective models III. The symplectic shell model of collective motion, Ann. Phys. **126**, 343 (1980).

[22] D. Rowe and G. Rosensteel, Rotational bands in the U(3)-boson model, Phys. Rev. C **25**, 3236 (1982).

[23] O. Castaños and J. Draayer, Contracted symplectic model with ds-shell applications, Nucl. Phys. A **491**, 349 (1989).

[24] J. Cseh, Semimicroscopic algebraic description of nuclear cluster states: Vibron model coupled to the SU(3) shell model, Phys. Lett. B **281**, 173 (1992).

[25] J. Cseh and G. Lévai, Semimicroscopic algebraic cluster model of light nuclei. I. Two-cluster-systems with spin-isospin-free interactions, Ann. Phys. **230**, 165 (1994).

[26] J. Cseh, Spontaneous symmetry-breaking in Elliott-type models and the nuclear deformation, Phys. Lett. B **793**, 59 (2019).

[27] J. Cseh, Dual breaking of symmetries in algebraic models, Eur. Phys. J. Spec. Top. **229**, 2543 (2020).

[28] P. Rochford and D. Rowe, The survival of rotor and SU(3) bands under strong spin-orbit symmetry mixing, Phys. Lett. B **210**, 5 (1988).

[29] D. J. Rowe, P. Rochford, and J. Repka, Dynamic structure and embedded representation in physics: The group theory of the adiabatic approximation, J. Math. Phys. **29**, 572 (1988).

[30] M. Jarrio, J. Wood, and D. Rowe, The SU(3) structure of rotational states in heavy deformed nuclei, Nucl. Phys. A **528**, 409 (1991).

[31] P. Hess, A. Algora, M. Hunyadi, and J. Cseh, Configuration-mixed effective SU(3) symmetries, Eur. Phys. J A **15**, 449 (2002).

[32] D. Rowe, Microscopic theory of the nuclear collective model, Rep. Prog. Phys. **48**, 1419 (1985).

[33] A. Algora, J. Cseh, J. Darai, and P. Hess, Ternary clusterization and quadrupole deformation, Phys. Lett. B **639**, 451 (2006).

[34] J. Darai, J. Cseh, and D. G. Jenkins, Shape isomers and clusterization in the ^{28}Si nucleus, Phys. Rev. C **86**, 064309 (2012).